Journal of Molecular Catalysis A: Chemical 380 (2013) 118–130

Contents lists available at ScienceDirect

Journal of Molecular Catalysis A: Chemical

journal homepage: www.elsevier.com/locate/molcata

FTIR study of β-picoline and pyridine-3-carbaldehyde transformation on V–Ti–O catalysts. The effect of sulfate content on β-picoline oxidation into nicotinic acid

Yuriy A. Chesalov*, Tamara V. Andrushkevich, Vladimir I. Sobolev, Galina B. Chernobay

Boreskov Institute of Catalysis, Russian Academy of Sciences, Prosp. Lavrentieva, 5, Novosibirsk 630090, Russian Federation

ARTICLE INFO

Article history:
Received 1 July 2013
Received in revised form
19 September 2013
Accepted 20 September 2013
Available online 1 October 2013

Keywords:
Vanadia–titania catalysts
Sulfates
β-Picoline oxidation
Nicotinic acid
FTIR spectroscopy

ABSTRACT

Surface complexes of β-picoline, 3-pyridine-carbaldehyde and nicotinic acid on 20 wt.% V_2O_5/TiO_2 catalysts containing 0.07 and 6.31 wt.% SO_4^{2-} were studied by FTIR spectroscopy and temperature programmed reaction technique. The water (both H_2O and D_2O), pyridine and β-picoline were used as molecular probes for identification of surface acidity and the structure of sulfate species. Both samples possess Lewis and Brönsted acidic sites. β-Picoline, 3-pyridine-carbaldehyde and nicotinic acid form surface complexes of similar structure on both studied catalysts. But high sulfated catalyst contains stronger Brönsted sites in greater amount. It leads to the formation of stronger bound surface complexes of β-picoline, 3-pyridine-carbaldehyde and nicotinic acid. The strongly bound surface complexes are transformed into by-products (CO_x, pyridine and 3-cyanopyridine). It resulted in substantial reduction of nicotinic acid yield.

1. Introduction

Vapor-phase oxidation of β-picoline by oxygen from the air is a promising “green chemistry” approach for developing a technology for the nicotinic acid production [1,2]. Nicotinic acid is widely used in medicine, cosmetics, food industry, agriculture, and as a monomer for various organic syntheses. Currently the global annual nicotinic acid production exceeds 40 000 tons.

A novel method for the nicotinic acid production by single-stage β-picoline oxidation with oxygen from the air in the presence of water over a vanadia–titania oxide catalyst was developed at Boreskov Institute of Catalysis SB RAS in the early 90s [3–5]. The catalyst synthesis method uses the titanium oxide support that is industrially produced by the sulfate technology. Such material contains up to 10 wt.% SO_4^{2-}.

As it was demonstrated by us earlier [6], the FTIR spectra reveal differences in the type, quantity and strength of acid sites as well as in the composition and strength of surface complexes of β-picoline, 3-pyridine-carbaldehyde and nicotinic acid as a function of the SO_4^{2-} content in the anatase TiO_2. The surface aldehyde and nicotinate complexes become dead-end forms on high sulfated TiO_2. Meanwhile, such complexes are weakly bound on low sulfated TiO_2 and are easily desorbed in the original form. The pronounced SO_4^{2-} effect on the properties of the support makes it important to study the effect of the sulfate content in supported vanadia–titania catalysts on their acidity and adsorption properties as well as their catalytic performance in the β-picoline oxidation.

The acid–base characteristics of the oxide material have three major effects on the selective oxidation of hydrocarbons. They affect the reactant molecule activation, the rates of competitive transformation pathways and the rates of adsorption and desorption of the reactants and products [7].

The effect of the acid-base properties is clearly revealed under the catalyst promotion with basic (K, Na, Cs, Li) or acidic (P, W, SO_4^{2-}) agents. The alkali doping of V_2O_5/TiO_2 catalysts for the oxidative dehydrogenation of propane resulted in the decrease of the acidity and increase of the basicity of the active centers. The increase in the selectivity was ascribed to easier propene desorption from the less acidic surface, preventing the consecutive propene combustion [8–10].

Modification of V_2O_5/TiO_2 catalysts with sulfate results in growing acidity and promotes methanol oxidation to dimethoxymethane (DMM) [11–14].

For oxidation of C_1–C_4 aldehydes to acids it was demonstrated that the acid-base properties of the catalysts strongly affect the direction of aldehydes transformation into the acids or deep oxidation products. An increase of the V–Mo catalyst acidity by doping with phosphorus increases the strength of the surface aldehyde complexes, their conversion to deep oxidation products and lowers the selectivity to acids. Promotion with bases leads to higher

---

* Corresponding author. Tel.: +7 383 330 72 84; fax: +7 383 3308056.
E-mail address: chesalov@ngs.ru (Y.A. Chesalov).

1381-1169/$ – see front matter © 2013 Elsevier B.V. All rights reserved.
http://dx.doi.org/10.1016/j.molcata.2013.09.028

basicity and decreases the selectivity due to the formation of strongly adsorbed forms of the acids [15,16].

Acid-base properties of catalysts are an important factor in selective conversion of methyl aromatics and hetero aromatics. Martin [17] demonstrated that the oxidation of these hydrocarbons to their aldehydes strongly depends on the nature, strength and concentration of acid and base surface sites of the catalysts and the acid–base properties of the reaction mixture. On promoted vanadium catalysts the selectivity to substituted benzaldehydes is closely related to the basic properties of the catalyst whereas the activity strongly depends on the amount and strength of acid sites. The selectivity of vanadium-containing catalysts to aldehydes obtained from methyl- and hetero aromatic compounds (including isomeric picolines) can be increased by adding alkaline cations or organic bases blocking strong acid sites [17]. For toluene oxidation the increase of the basicity of V–Ti catalysts doped with potassium improves the selectivity to benzyl aldehyde and decreases the selectivity to benzoic acid [18,19]. Kalevaru et al. [20] determined that the highest possible acidity in a series of V_2O_5/MgF_2 catalysts is required for selective oxidative ammonolysis of β-picoline to nicotinonitrile.

Takehira et al. [21] studied the effect of the acidity of $CrV_{1-x}P_xO_4$ catalysts on their activity in β-picoline oxidation and selectivity to nicotinic acid. NH_3-TPD and infrared study of adsorbed pyridine showed an increase in the concentration of Lewis and Brönsted acid sites through replacing V with a small amount of P in $CrVO_4$. It was found that the addition of P ($x < 0.1$) in monoclinic $CrVO_4$ enhanced the catalytic activity due to the cooperation between the acid sites and the redox properties of VO_4. An increase of the selectivity was related by the authors to higher acidity. The higher acidity enhances the selectivity, probably, due to better desorption of the formed acid and prevention of its re-adsorption, thus, protecting the acid from deep oxidation [21,22].

Modification of vanadia–titania catalysts with sulfates substantially alters their acid and redox properties. Sulfated catalysts have Lewis and Brönsted acid sites. The concentration and ratio of the Lewis and Brönsted sites depends on the SO_4^{2-} content [23], the amount, type and dispersion of vanadia [12,14,24–26], type of sulfate species [13], and temperature of the catalyst heat treatment [23–25]. Lewis sites are transformed into Brönsted sites at higher of SO_4^{2-} and water vapor contents, and decreasing calcination temperatures.

Heinz et al. [27] studied vanadia–titania catalysts prepared using anatase TiO_2 containing 0.5–1.5 wt.% SO_4^{2-}. The authors concluded that variation of the sulfate content in this range did not have a significant effect on the acidity and catalytic properties in β-picoline oxidation. However, in another paper of the same group the nicotinic acid yield was found to decrease from 84 to 74% when the sulfate content was increased from 0.5 to 1.5 wt.% [28]. The highest nicotinic acid yield (97%) was observed in this study over a catalyst supported on TiO_2 with 0.5 wt.% SO_4^{2-} [28].

The current study is devoted to the investigation of vanadia–titania catalysts with substantially different sulfate content to elucidate clearly effect of SO_4^{2-} content on the mechanism of β-picoline oxidation.

2. Experimental

2.1. Samples preparation

TiO_2 was prepared from a commercial (Euro Support Manufacturing Czechia) titanium hydroxide obtained by thermal hydrolysis of a titanyl sulfate. The initial product contained 88% anatase modification of titania. A solid hydrogel was separated by decantation from the initial aqueous suspension, washed with water to remove SO_4^{2-} to a certain content of SO_4^{2-}. An aqueous solution of vanadyl oxalate was added to the paste. Slurry was dried in lab spray-dryer (Buchi-290). Then the samples were calcined in air at 450 °C.

2.2. Samples characterization

Analysis of the sulfur content was performed by X-ray fluorescence spectrometry on an ARL-Advant'X analyzer with Rh anode of the X-ray tube. Qualitative analysis of sulfate forms was performed by FTIR spectroscopy. Infrared spectra of the samples (4000–200 cm^{-1}, 30 scans, resolution 4 cm^{-1}) were obtained on BOMEM MB-102 FTIR spectrometer by standard technique – pressing with CsI (2 mg and 500 mg CsI).

X-ray diffraction experiments were carried out on a Siemens D-500 diffractometer with a monochromated CuKα radiation. FT-Raman spectra (3600–100 cm^{-1}, 300 scans, resolution 4 cm^{-1}, 180° geometry) were recorded using a RFS 100/S spectrometer (Bruker). Excitation of the 1064 nm line was provided by an Nd-YAG laser (100 mW power output).

2.3. In situ FTIR experiments

In situ FTIR experiments were performed in a flow IR cell reactor with a BOMEM MB-102 FTIR spectrometer. The sample powder (35–50 mg) was pressed into a self-supported 1 cm × 3 cm wafer. The wafer was mounted into a quartz IR cell reactor with CaF_2 windows and activated in an air flow (50 cm^3/min) at 300 °C for 60 min.

To study the effect of water a mixture of 4%H_2O (or D_2O) in air was introduced to the IR cell with VTi sample at 100–350 °C.

β-Picoline used for the adsorption was $C_5H_4NCH_3$ from Aldrich Chemical Company, Inc. (purity 99%). Pyridine-3-carbaldehyde used for the adsorption was C_5H_4NCHO from Aldrich Chemical Company, Inc. (purity 99%). The adsorption was carried out at 90–250 °C by injecting β-picoline or pyridine-3-carbaldehyde (1–2 μl) into air flowing through the IR cell reactor. 1–2 μg of crystalline nicotinic acid C_5H_4NCOOH (home-made sample obtained according [3], purity 99.8%) was introduced into air flow at 250 °C (temperature of nicotinic acid desublimation is 237 °C). All feed pipelines were thermostated at 250 °C.

The background FTIR spectra of the samples were obtained at each temperature for their further subtraction from the spectra of species adsorbed on the samples.

2.4. Catalysts test

The temperature programmed gas-phase oxidation reactions were performed in a quartz tube flow reactor with an internal diameter of 6 mm, using shaped catalyst granules ($d = 0.25$–0.5 mm). 1 g of VTi-1 and 150 mg VTi-2 diluted with crumb quartz were used. The reactive gas mixture (β-picoline/O_2/He = 60 ml/min) was fed into the reactor filled with the catalyst; the reactor was operated under atmospheric pressure. The reaction temperature was measured inside the reactor (±1 °C) using a thermocouple inserted into the catalyst bed. The heating rate was 1 K/min. During the catalytic runs, gas samples were analyzed periodically by integrated online gas chromatography (GC) with a flame-ionization detector (to determine the β-picoline conversion and selectivity to pyridine, nicotinic acid, pyridine-3-carbaldehyde, 3-cyanopyridine) and a thermal conductivity detector (to determine the selectivity to carbon oxides).

Prior to the kinetic measurements, the catalysts were activated in the reactor at 400 °C in a flow of O_2/He (1:3) for 1 h. The reactor was then cooled to 200 °C and the feed was switched at this

Table 1
Physicochemical characteristics of the samples.

Sample	Content of V_2O_5, wt.%	Phase composition	BET, m^2/g	SO_4^{2-} content, wt.%
VTi-1	20	TiO_2 (anatase), V_2O_5	13	0.07
VTi-2	20	TiO_2 (anatase), V_2O_5	140	6.31

temperature to the reactive gas mixture for 20–30 min in order to reach steady-state initial conditions.

3. Results and discussion

3.1. Samples characterization

3.1.1. Bulk characterization

Physicochemical characteristics of the samples are listed in Table 1.

X-ray diffraction of VTi-1 and VTi-2 samples reveals TiO_2 of the anatase structure and orthorhombic vanadia phase. The VTi-2 sample with a higher content of SO_4^{2-} has a greater surface area. It appears that sulfate ions increase the surface area [29] and delay the crystallization and sintering upon calcination [26].

Raman spectra of VTi-1 and VTi-2 samples collected at room temperature are presented in Fig. 1. This figure also shows the Raman spectra of anatase and orthorhombic vanadium oxide. The spectra of VTi-1 and VTi-2 (Fig. 1, spectrum 3 and 4) are virtually coincided. The bands at 995, 702, 642, 517, 485, 404, 305, 285, and 145 cm^{-1} are observed in these spectra. The bands at 642, 517, 404 cm^{-1} are due to lattice vibrations of anatase TiO_2 (see Fig. 1, spectrum 2), whereas the bands at 995, 702, 485, 305, and 285 cm^{-1} are assigned to lattice vibrations of orthorhombic V_2O_5 (see Fig. 1, spectrum 1). The bands with the maximum close to 145 cm^{-1} are observed both in the spectrum of anatase and in the spectrum of orthorhombic vanadia. Therefore, the band at 145 cm^{-1} observed in the spectra of VTi-1 and VTi-2 catalysts is a superposition of the bands due to lattice vibrations of V_2O_5 and TiO_2. Thus, according to Raman spectroscopy, both samples consist of orthorhombic V_2O_5 and TiO_2 of anatase modification. The bands due to the vibrations of any sulfur-containing species are not detected in Raman spectra of the samples.

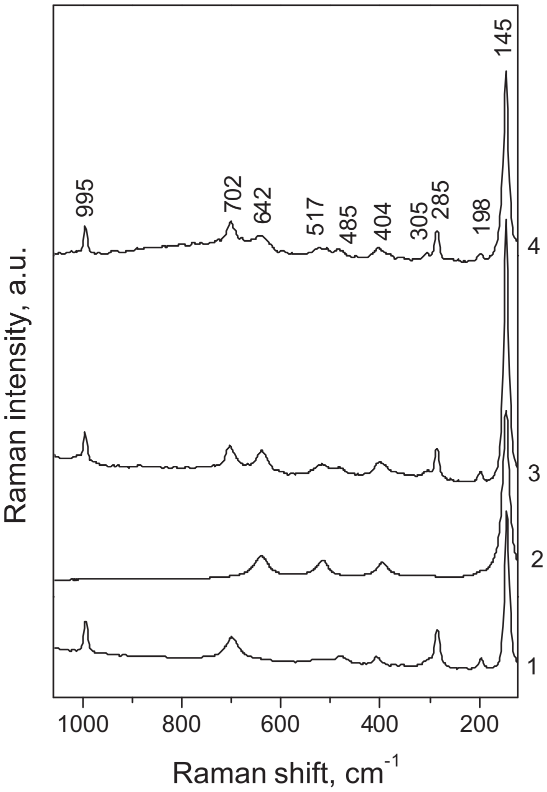

Fig. 1. Raman spectra of orthorhombic V_2O_5 (1), TiO_2 of anatase modification (2), VTi-1 (3), and VTi-2 (4).

FTIR spectra of VTi-1 and VTi-2 samples collected at room temperature are shown in Fig. 2. A broad band with a maximum at 3460 cm^{-1} is due to OH stretching vibrations of adsorbed water and hydrogen-bonded hydroxyl groups. The band at 1630 cm^{-1} characterizes the bend vibrations of the adsorbed water. The bands at ~1020, 820, 380 and 298 cm^{-1} are assigned to lattice vibrations of orthorhombic V_2O_5 [30], whereas a broad band at 900–400 and a band at 351 cm^{-1} are due to lattice vibrations of anatase modification of TiO_2 [31]. In addition, the bands at 1200–1100, 970 and 670 cm^{-1} due to asymmetrical (ν_3) and symmetrical (ν_1) stretching and asymmetrical bending (ν_4) modes of sulfate groups, respectively [32], are observed in the spectrum of VTi-2 catalyst. Three bands at 1153, 1124, and 970 cm^{-1} are observed in the region of $\nu(SO_4^{2-})$ vibrations. The first two bands are due to triply degenerate (for T_d symmetry) ν_3 mode. The latter band is due to the totally symmetric ν_1 mode (forbidden in the IR spectrum for the T_d symmetry) [32]. The splitting of ν_3 vibration into two components and the appearance of band due to ν_1 vibration in the infrared spectrum indicates monodentate mode of coordination and C_{3v} symmetry for SO_4^{2-} ion [32] in VTi-2 sample. The structures of mono- and bidentate sulfate complexes are shown in Fig. 3. Previously, we have shown in [6] that SO_4^{2-} ions are bidentately coordinated to titanium cations in the case of sulfated anatase TiO_2 samples. Bridging coordination of sulfate ions is detected at a low sulfur content (0.12 wt.%, $S = 195\ m^2/g$), whereas chelate coordination of SO_4^{2-} is observed at a large sulfur content (6.9 wt.%, $S = 300\ m^2/g$). In the case of VTi-2 sample (6.3 wt.%, $S = 140\ m^2/g$) sulfate ions are monodentately coordinated. The bands due to sulfate species are not observed in the spectrum of VTi-1 sample because of low concentration of SO_4^{2-}.

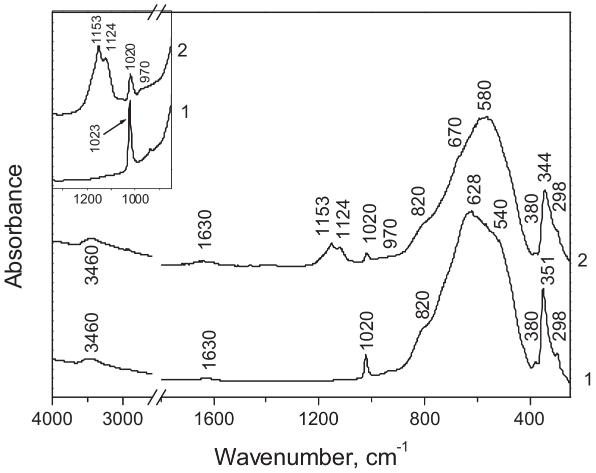

Fig. 2. FTIR spectra of VTi-1 (1) and VTi-2 (2) collected at ambient condition.

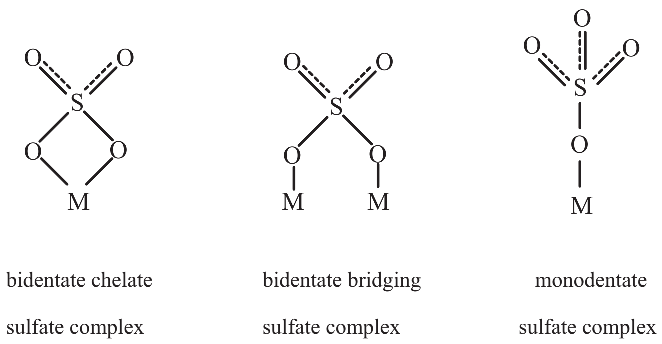

Fig. 3. The structure of bidentate and monodentate sulfate complexes [32].

3.1.2. Surface characterization

The state of the surface was studied by IR spectroscopy using molecular probes (water and β-picoline). Water as a molecular probe was used for the characterization of sulfate groups, whereas β-picoline was used as basic molecular probe for the characterization of Lewis and Brönsted acidity of the samples. It should be noted that VTi-1 and VTi-2 catalysts in the form of self-supported wafer are transparent only in the region 2200–1200 cm^{-1}. The opacity of the samples in the low-frequency region is caused by the strong absorption due to lattice modes of titania and vanadia. The opacity of the samples in the high-frequency region is due to the strong scattering caused by optical heterogeneity related to two-phase character of the samples.

To study the effect of water a gas mixture of 4%H_2O in air was passed through a cell with the sample at 100–350 °C. Fig. 1 shows the spectra of vanadia–titania catalysts collected after activation at 350 °C in dry air flow for 1 h. There is only a very weak band at 2030 cm^{-1} due to the first overtone of ν(V=O) vibration in the spectrum of VTi-1 sample (Fig. 4, spectrum 1). The bands at 2030 (ν(V=O)), 1620 ($\delta(H_2O)$), 1360 and 1285 cm^{-1} (ν(S=O) of surface sulfate groups [29,33,34]) are observed in the spectrum of VTi-2 sample (Fig. 4, spectrum 2). According to [35] the appearance of bands in the frequency range 1400–1300 cm^{-1} is typical for sulfated oxides such as ZrO_2, Al_2O_3 and TiO_2 and indicates covalently bound sulfate species. In our case it is impossible to identify reliably the coordination mode of covalently bound sulfate because of the impossibility collecting the full infrared spectrum due to the strong absorption of the samples below 1200 cm^{-1} caused by anatase and vanadia lattice vibrations.

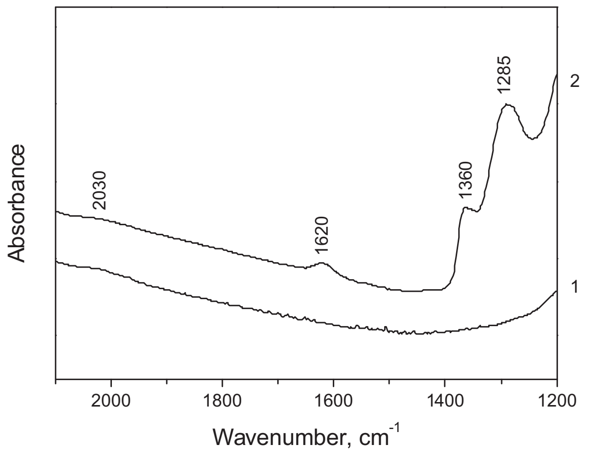

Fig. 4. FTIR spectra of VTi-1 (1) and VTi-2 (2) registered after 1-h activation at 350 °C in dry air.

When the amount of adsorbed water is increased there are some changes in the IR spectra (Fig. 5). In the case of VTi-1 sample (Fig. 5, spectrum 1) there is only an increase in the intensity of $\delta(H_2O)$ band at 1640 cm^{-1}. In the case of VTi-2 sample (Fig. 5, spectrum 2) there is a change also in the spectrum of sulfate groups. The frequency of the band at 1360 cm^{-1} is reduced by ~30 cm^{-1}, and its intensity is also reduced. Simultaneously, the intensity of the band at 1285 cm^{-1} is decreases, and its frequency is gradually reduced to 1230 cm^{-1}. Perhaps this is due to fact that two processes run simultaneously: symmetrization of SO_4 tetrahedron leading to a decrease in ν(S=O) frequency and a change in the mode of sulfate group coordination resulting in a decrease in ν(S=O) band intensity. One can also assume that the formation of monodentate sulfate groups occurs with increasing amount of adsorbed water and hydroxyl groups on the surface of the catalyst. As shown above (see Fig. 2) monodentate sulfate, which is the main form in the case of the fully hydrated

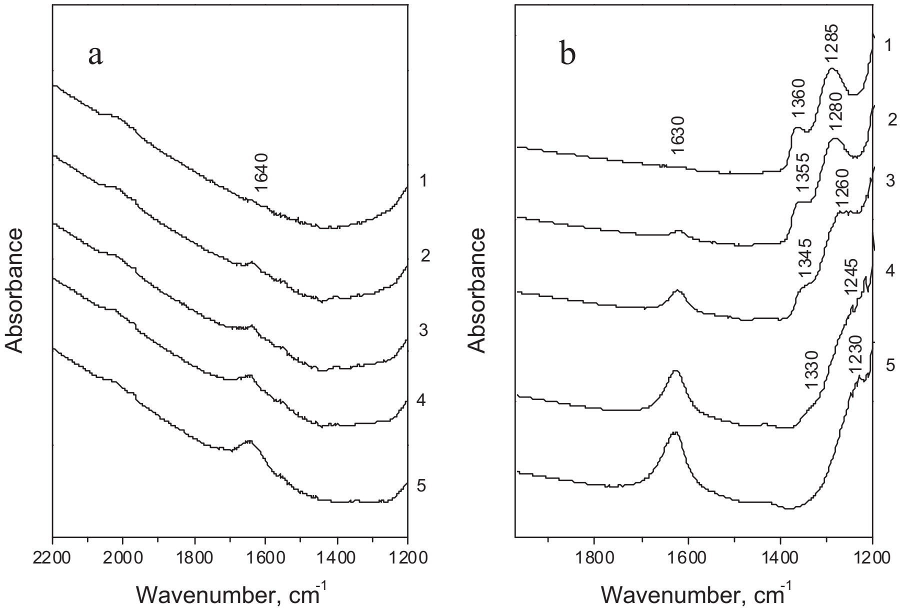

Fig. 5. FTIR spectra collected during passing a gas mixture 4%H_2O in air through IR cell with VTi-1 (a) and VTi-2 (b) sample at 350 °C (1), 300 °C (2), 250 °C (3), 200 °C (4), and 100 °C (5).

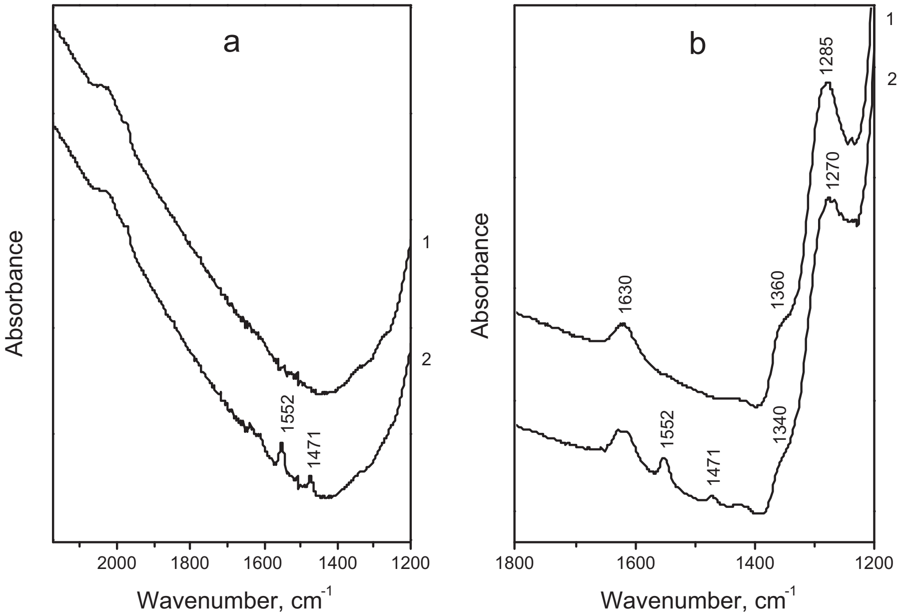

Fig. 6. FTIR spectra of VTi-1 (a) and VTi-2 (b) collected in dry air (1) and after 0.2 μl β-picoline adsorption (2) at 100 °C.

VTi-2 sample, is characterized by the bands at 1153, 1124, 970, and 670 cm^{-1}. In this case (the experiments described in Fig. 5b) the sample were pressed into self-supported wafers and there is almost complete absorption of infrared radiation in 1200–600 cm^{-1} region due to the lattice modes of anatase and vanadia. Thus, the hydration of VTi-2 sample results in the change in symmetry of SO_4 tetrahedron and in the mode of sulfate ions coordination.

We used β-picoline as a molecular probe to study the strong Brönsted and Lewis acidity of vanadia–titania catalyst. The centers capable to protonate the weak bases are considered as strong Brönsted acid sites. The adsorption of β-picoline was carried out at low temperature (100 °C) to avoid its oxidation. It should be noted that in our work β-picoline was also employed as a reactant.

Fig. 6 shows FTIR spectra of VTi-1 and VTi-2 collected in dry air and after β-picoline adsorption at 100 °C. Fig. 7 shows difference FTIR spectra of β-picoline adsorbed on VTi-1 and VTi-2 at 100 °C. The spectrum 1 in Fig. 7 is the difference between the spectra 2 and 1 presented in Fig. 6a. The spectrum 2 in Fig. 7 is the difference between the spectra 2 and 1 demonstrated in Fig. 6b. Thus, the spectra shown in Fig. 7 are due to surface species of β-picoline. The bands at 1633, 1613, 1552 and 1471 cm^{-1} due to ν(CC, CN) modes of the 3-methylpyridinium ion [36–38] is observed in these spectra. This surface complex is formed by the interaction of β-picoline molecule with a strong Brönsted acid site of the catalyst. There are no bands due β-picoline complexes with Lewis acid sites of catalysts in the registered spectra. The intensity of the bands due to 3-methylpyridinium ion is ~twofold in the spectrum 2 as compared with the spectrum 1 (Fig. 7). The same volume of β-picoline (0.2 μl) was injected into a cell with a catalyst in experiments shown in Figs. 6 and 7. This amount was sufficient to completely cover the surface of the catalyst VTi-1, but not enough to completely fill VTi-2 surface. The amounts of β-picoline enough to fill the surface of both catalysts were evaluated under static conditions. A small volume of β-picoline (0.02 μl) was injected into the cell with VTi-1 or VTi-2 samples at 100 °C. This resulted in the appearance of the bands of 3-methylpyridinium ion in the spectra of both catalysts. The procedure was repeated several times until a constant value of intensity of the bands due to 3-methylpyridinium ion was achieved. The concentration of strong Brönsted acid cites was calculated taking into account total amount of adsorbed β-picoline, catalyst weight and a specific surface. The concentration of the centers is 35 μmol/g (2.7 μmol/m^2) in VTi-1 catalyst and 190 μmol/g (1.4 μmol/m^2) in VTi-2. The surface concentration of these centers is less in the VTi-2 catalyst probably due to unavailability of micropore volume for adsorption of rather bulk molecule of β-picoline. The specific surface of micropores is about 70% of the total surface of the sample. In the case of VTi-2 sample 3-methylpyridinium ion formation is accompanied by a low-frequency shift of ν(S=O) bands of surface sulfate species for 15–20 cm^{-1} (Fig. 6b) due to the symmetrization of SO_4-group and the change in strength of Ti–O(S) bond. Thus, at least part of strong Brönsted acid sites is associated with the presence of sulfate ions on the surface of VTi-2.

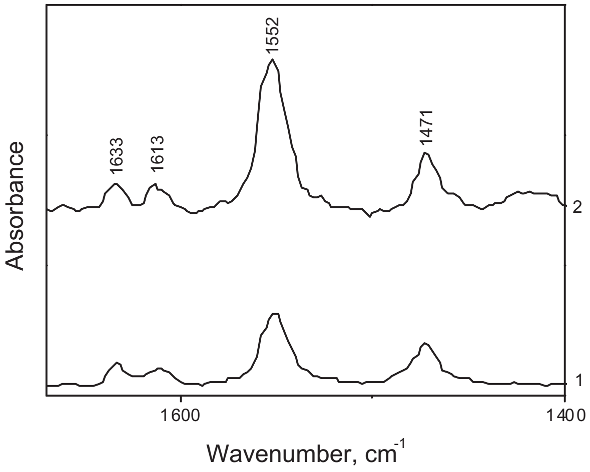

Fig. 7. Difference FTIR spectra of 0.2 μl β-picoline adsorbed on VTi-1 (1) and VTi-2 (2) at 100 °C.

As indicated above, self-supported wafers of vanadia–titania catalysts used in this study are transparent only in the region 2200–1200 cm^{-1}. The opacity of the samples in the high-frequencies region limits the opportunities for studying the structure of the catalyst surface sites. To obtain the additional information a model vanadia–titania catalyst was also examined. This catalyst was synthesized by the same technique but calcined at 400 °C rather than at 450 °C. The sulfur content in it is the same as in the catalyst VTi-1. This sample has better optical characteristics

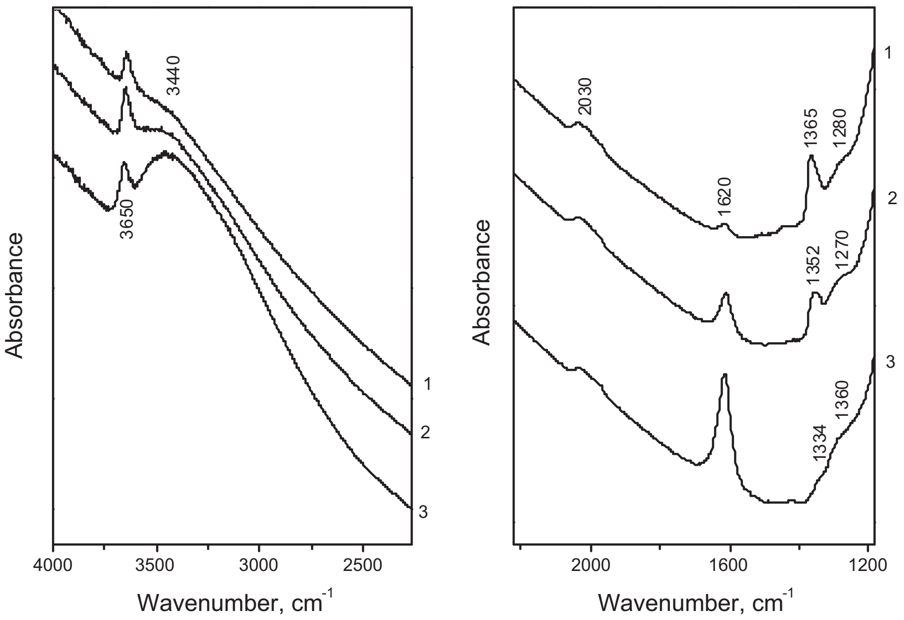

Fig. 8. FTIR spectra collected during passing a gas mixture 4%H_2O in air through IR cell with model VTi catalyst at 250 °C (1), 150 °C (2), and 100 °C (3).

and is sufficiently transparent in the 4000–1200 cm^{-1} spectral region. It allows measuring a spectrum of hydroxyl groups.

Fig. 8 demonstrates the spectrum of model VTi catalyst collected after 1-h activation of the sample in dry air flow at 250 °C (spectrum 1). The bands at 3650, 3440, 2030, 1620, 1365, and 1280 cm^{-1} are observed in the spectrum. The band at 3650 cm^{-1} is due to the OH stretching vibration of the surface hydroxyl group bound to two surface V atom (type II) [39]. The broad band at 3700–2700 cm^{-1} with a maximum at 3440 cm^{-1} ($\nu_{as}(H_2O)$ and $\nu_s(H_2O)$) and the band at 1620 cm^{-1} ($\delta(H_2O)$) characterize the adsorbed water. The band at 2030 cm^{-1} is assigned to the first overtone of ν(V=O) mode. The bands at 1360 and 1285 cm^{-1} characterize surface covalently bound sulfate species (ν(S=O) mode) [29,33,34].

When the amount of adsorbed water is increased there are significant changes in the IR spectra (Fig. 8, spectra 2 and 3). Increasing the concentration of the adsorbed water (bands at 3440 and 1620 cm^{-1}) is accompanied by an increase in the concentration of surface hydroxyl groups (3650 cm^{-1}). There is also a change in the spectrum of sulfate groups. A gradual low-frequency shift (∼20–30 cm^{-1}) of ν(S=O) bands at 1365 and 1280 cm^{-1} is observed and their intensity is also decreased. As mentioned above, this is caused by two processes taking place simultaneously. The symmetrization of SO_4 tetrahedron results in decrease of the frequency of ν(S=O) vibrations, and the change of coordination mode of sulfate ion lead to decrease in the intensity of ν(S=O) bands. Both of these processes are due to the increasing number of hydroxyl groups and water molecules coordinated to surface vanadium cations.

To further characterize the acid sites of the catalyst the proton-containing groups were exchanged by a deuterium. β-Picoline was used as a molecular probe to study the Brönsted and Lewis acidity of vanadia–titania catalyst.

Passing a gas mixture 4% D_2O in air through IR cell with a model VTi catalyst at 200 °C for 15 min results in the disappearance of the bands at 3650 (ν(OH)), 3440 ($\nu(H_2O)$) and 1620 ($\delta(H_2O)$) cm^{-1} and the simultaneous appearance of new bands at 2685 (ν(OD)) and 2540 ($\nu(D_2O)$) cm^{-1} (Fig. 9). At the same time, the replacement of protons by deuterium results in only minor shift of ν(S=O) bands of sulfate species. However, there is a clear effect of the concentration of hydroxyl groups and adsorbed water on the frequencies of ν(S=O) vibrations (Fig. 8). Thus, hydroxyl group is not directly bound to S atoms of sulfate groups, but is coordinated to vanadium ions. The first coordination sphere of these vanadium ions also includes the oxygen atoms of sulfate groups. Hydroxyl group also could be bound to the neighboring vanadium ions. The minor shift of ν(S=O) bands of sulfate species caused by H-D exchange could be due to the formation of hydrogen bonds between the protons of adsorbed water molecules (or the surface-OH groups) and oxygen of sulfate groups.

Adsorption of β-picoline on model VTi catalyst containing OH-groups (Fig. 10, spectrum 1) results in a decrease in intensity of the band at 3650 cm^{-1} of surface OH-group (the band has negative intensity in difference spectrum). Simultaneously, the bands at 3400–1800 (ν(NH···O), 3125, 3080 and 3047 (ν(CH) of pyridine ring), 2936 and 2885 ($\nu(CH_3)$), 1633, 1613, 1552, and 1471 (ν(CC, CN)), and 1390 ($\delta(CH_3)$) cm^{-1} assigned to the vibrations of 3-methylpyridinium ion [36–38] appear in the spectrum (Fig. 10,

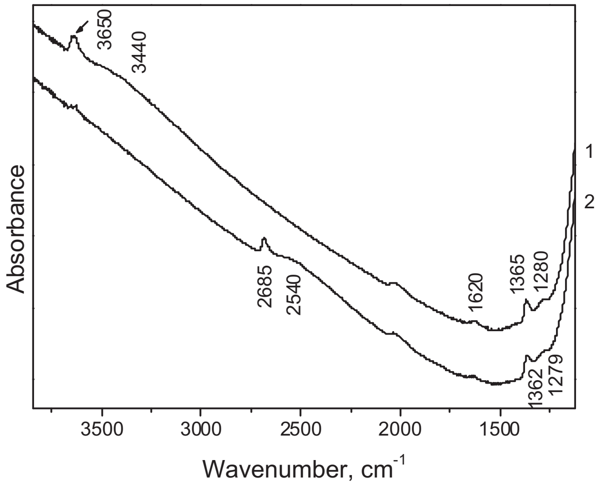

Fig. 9. FTIR spectra of model VTi catalyst at 200 °C collected after 1-h activation in dry air (1) and after passing a gas mixture 4%D_2O in air through IR cell during 15 min (2).

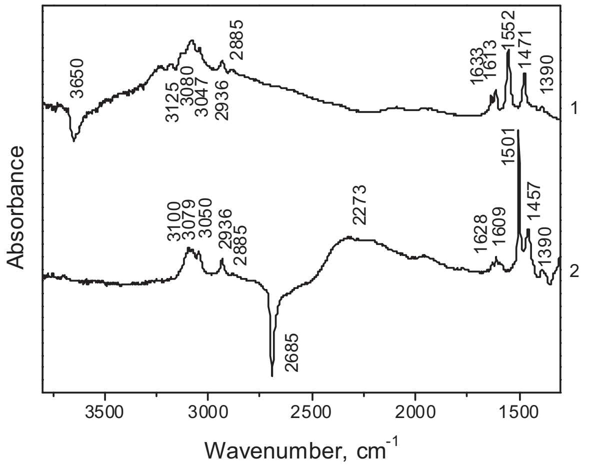

Fig. 10. Difference FTIR spectra of β-picoline adsorbed at 100 °C on model VTi catalyst containing OH- (1) and OD- (2) groups.

spectrum 1). This surface complex is formed by the interaction of β-picoline molecule with a strong Brönsted acid site of the catalyst.

Adsorption of β-picoline on model VTi catalyst containing OD-groups (Fig. 10, spectrum 2) results in a decrease in intensity of the band 2685 cm^{-1} of surface OD-groups. The bands at 3100, 3079 and 3050 (ν(CH) of pyridine ring), 2936 and 2885 ($\nu(CH_3)$), 2500–1800 (ν(ND$\cdots$O), 1628, 1609, 1501, and 1457 (ν(CC, CN)), and 1390 ($\delta(CH_3)$) cm^{-1} are observed in the spectrum of deuterated analog of 3-methylpyridinium ion. The bands of ν(NH$\cdots$O) (shift ~800 cm^{-1}) and ν(CC, CN) at 1552 cm^{-1} (shift ~50 cm^{-1}) vibrations are the most sensitive to H-D exchange in the measured spectral region. It is clear that ν(CC, CN) vibration is coupled. Deuteration induced low-frequency shift of ν(CC, CN) band is apparently due to the contribution of δ(NH) vibration into this coupled mode. The concentration of surface hydroxyl groups of model VTi catalyst (OH or OD) decreases after the formation of 3-methylpyridinium ion (or it deuterated analog). Other β-picoline surface complexes under these conditions are not formed. Thus, the surface OH (or OD) groups are strong Brönsted acid sites of vanadia–titania catalysts. Fig. 8 demonstrates that increasing the amount of adsorbed water increases the number of hydroxyl groups. And, therefore, should also increase the number of strong Brönsted acid sites. It is also known that water significantly affects the rate of β-picoline oxidation on VTi catalyst and selectivity to nicotinic acid [1]. We have studied the effect of the amount of adsorbed water on the acidity of the model VTi catalyst. The research was carried out at 250 °C. This temperature is close to the optimum for the oxidation of β-picoline into nicotinic acid on vanadia–titania catalysts. Due to fast oxidation under such conditions β-picoline cannot be used as a molecular probe. Therefore, we used a pyridine. Fig. 11a demonstrates a FTIR spectra of model VTi catalyst collected at 250 °C after 1-h activation in dry air flow at 300 °C (spectrum 1) and after H_2O adsorption at 250 °C (spectrum 2). The bands at 3650 cm^{-1} due to ν(OH) mode of surface hydroxyl groups and 1365 cm^{-1} assigned to ν(S=O) vibration of surface sulfate groups are observed in the spectrum of model VTi catalyst before water adsorption. Adsorption of water results in ~50% increase in intensity of ν(OH) band, low-frequency shift of ν(S=O) band and an appearance of the bands at 3440 and 1620 cm^{-1} due to adsorbed water. Pyridine adsorption results in the appearance of bands at 1635, 1606, 1536, 1486 and 1447 cm^{-1} in the spectrum of dehydrated sample. The bands at 1635 and 1536 cm^{-1} are assigned to vibrations of pyridinium ion formed by interaction of pyridine with a strong Brönsted acid sites of the catalyst, the band at 1447 cm^{-1} characterize surface complex of pyridine with a Lewis acid sites of the catalyst, whereas the bands at 1606 and 1486 cm^{-1} could be assigned to both surface complexes [40]. Adsorption of pyridine after water pre-adsorption results in ~40% increase in the intensity of bands due to pyridinium ion and ~70% decrease in the intensity of band due to surface complex of pyridine with Lewis acid sites. Thus, the adsorption of water increases the amount of Brönsted acid sites and reduces the amount of Lewis acid sites. At the same time, increasing number of Brönsted acid sites (40%) correlates well with the increase in concentration of surface hydroxyl groups (50%).

Thus, surface hydroxyl groups bound to vanadium ions are the strong Brönsted acid sites of studied vanadia–titania catalysts. Sulphate ions are coordinated to the same vanadium ions as a hydroxyl

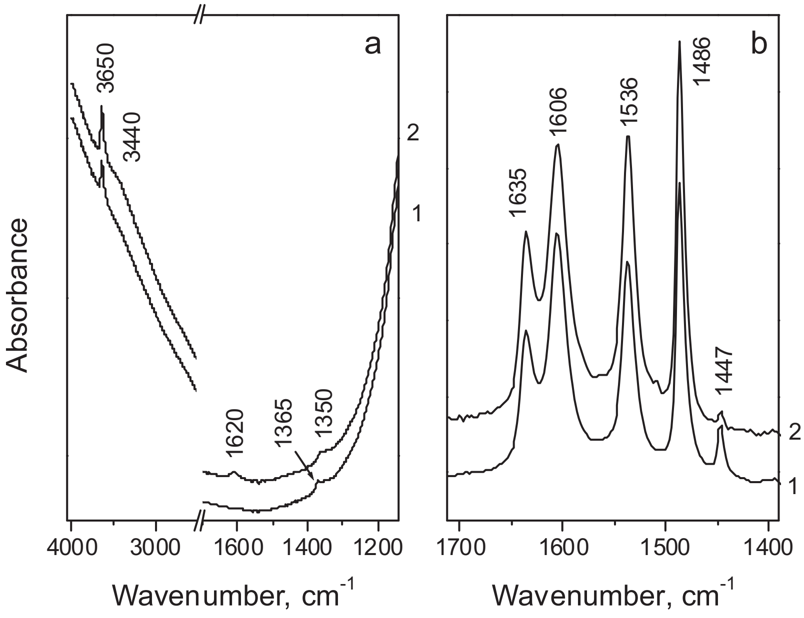

Fig. 11. (a) FTIR spectrum of model VTi catalyst collected at 250 °C after 1-h activation in dry air flow at 300 °C (1) and FTIR spectrum of the same catalyst after H_2O adsorption at 250 °C (2). (b) Difference FTIR spectra of pyridine adsorbed at 250 °C on model VTi catalyst after 1-h activation in dry air flow at 300 °C (1) and after H_2O adsorption at 250 °C (2).

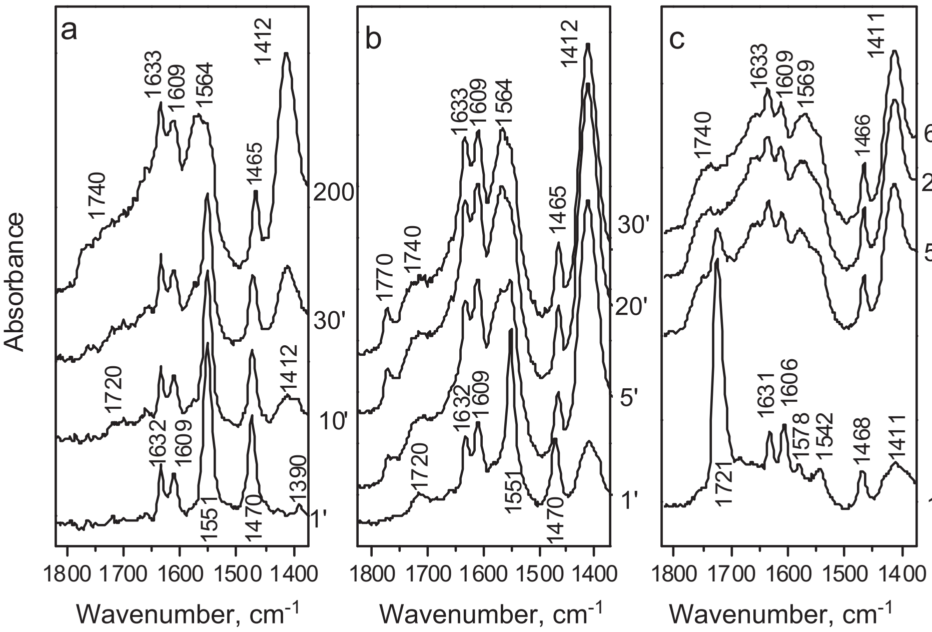

Fig. 12. The difference FTIR spectra collected after introduction of β-picoline at 200 °C (a) and 250 °C (b) and pyridine-3-carbaldehyde at 160 °C (c) in the cell with VTi-1 catalyst.

group or to the neighboring vanadium ions. As a result, sulfate ions can modify the Brönsted acidity of vanadia–titania catalysts. Furthermore, for the same reasons sulfate ions can also modify Lewis acidity of the catalysts. The adsorption of water increases the number of Brönsted acid sites and reduces the amount of Lewis acid sites due to the formation of additional hydroxyl groups. The structure of sulfate complexes (the mode of coordination and the symmetry of SO_4 tetrahedron) is also determined by the number of surface hydroxyl groups and adsorbed water. Thus, there is a mutual influence of sulfate groups and protic acid centers.

3.1.3. *Transformation of β-picoline and pyridine-3-carbaldehyde on vanadia–titania catalysts*

The study of the interaction of β-picoline with VTi-1 and VTi-2 catalysts was carried out at two temperatures (200 and 250 °C). The interaction of pyridine-3-carbaldehyde with the same catalysts was studied at 160 °C. Selecting a relatively low temperature for the investigation of pyridine-3-carbaldehyde transformation was caused by the high rate of it transformation on VTi catalysts at temperatures above 200 °C. It makes impossible studying the dynamics of changes in the spectra.

Fig. 12 demonstrates the difference FTIR spectra collected after introduction of β-picoline at 200 °C (a) and 250 °C (b) and pyridine-3-carbaldehyde at 160 °C (c) in the cell with VTi-1 catalyst.

The bands at 1632, 1609, 1551, 1474 (ν(CC, CN)) and 1390 ($\delta(CH_3)$) cm^{-1} due to 3-methylpyridinium ion [36–38] (Table 2, SC1) are observed in the spectrum registered at 200 °C in 1 min after introduction of β-picoline (Fig. 12a). As indicated in Section 3.1.2, this surface complex is formed by interaction of β-picoline with strong Brönsted acid centers of vanadium–titanium oxide catalysts. The bands at 1720 cm^{-1} due to ν(C=O) vibration of pyridine-3-carbaldehyde surface complex [41] (Table 2, SC2) and at 1412 cm^{-1} assigned to ν_s(COO) mode of nicotinate surface complex [36] (Table 2, SC3) are appeared in the spectrum 10 min after the introduction of β-picoline. With time the intensity of bands at 1412 cm^{-1} increases. The second band of niconitate complex at 1564 cm^{-1} (ν_{as}(COO) is manifested in the spectra. And the band at 1740 cm^{-1} due to ν(C=O) vibration of molecular adsorbed nicotinic acid (Table 2, SC4) [36] is also appeared in the spectra.

The transformation of 3-methylpyridinium ion proceeds significantly faster at 250 °C (Fig. 12b), than at 200 °C (Fig. 12a). The bands due to vibration of surface pyridine-3-carbaldehyde and nicotinate are observed in the spectrum collected only 1 min after introduction of β-picoline. After 5 min, the bands due to ν(C=O) mode of molecularly adsorbed (1740 cm^{-1}) and gaseous (1770 cm^{-1}) nicotinic acid [6] are appeared in the spectrum.

The bands at 1721 (ν(C=O)), 1631, 1606, 1578, 1542, 1468 (ν(CC, CN)), and 1411 (ν_s(COO)) cm^{-1} are observed in the spectrum registered at 160 °C in 1 min after introduction of pyridine-3-carbaldehyde (Fig. 12c). The value of the frequency due to ν(C=O) vibration indicates the formation of hydrogen bonds between pyridine-3-carbaldehyde molecule and Brönsted acid site of VTi-1 catalyst through oxygen of a carbonyl group [41]. The bands at 1631, 1606, 1542, and 1468 cm^{-1} are assigned to substituted pyridinium ions [36–38]. The presence of ν(CC, CN) band at 1578 cm^{-1} in the spectrum indicates the interaction of the molecule pyridine-3-carbaldehyde with a Lewis acid centers via an unshared electron pair of pyridine ring nitrogen [42–45]. Thus, we can assume that two surface complexes of pyridine-3-carbaldehyde are formed (Table 3, SC2 and SC5). In addition, the band at 1411 cm^{-1} due to ν_s(COO) mode of nicotinate surface complex (Table 3, SC3) is also observed in the spectrum. With time the intensity of ν(C=O) band at 1721 cm^{-1} due to surface complexes of pyridine-3-carbaldehyde is reduced and the intensity of bands due to nicotinate surface complex at 1569 and 1411 cm^{-1} is increased. The band at 1740 cm^{-1} due to ν(C=O) mode of molecular adsorbed nicotinic acid (Table 3, SC4) is also appeared in the spectrum.

Fig. 13 demonstrates difference FTIR spectra collected after the introduction of β-picoline at 200 °C (a) and 250 °C (b) and pyridine-3-carbaldehyde at 160 °C (c) into the cell with VTi-2 catalyst. The bands at 1633, 1612, 1553, and 1472 cm^{-1} assigned to ν(CC, CN) vibrations of 3-methylpyridinium ion (Table 2, SC1) are observed in the spectrum registered at 200 °C within 1 min after introduction of β-picoline into the cell with VTi-2 catalyst (Fig. 13a). In 10 min after β-picoline introduction, the spectrum reveals a new band at 1418 cm^{-1} due to ν_s(COO) vibration of surface nicotinate complex (Table 2, SC3). The ν(C=O) bands at 1740 and 1670 cm^{-1} of two forms of molecular adsorbed nicotinic acid are also observed in

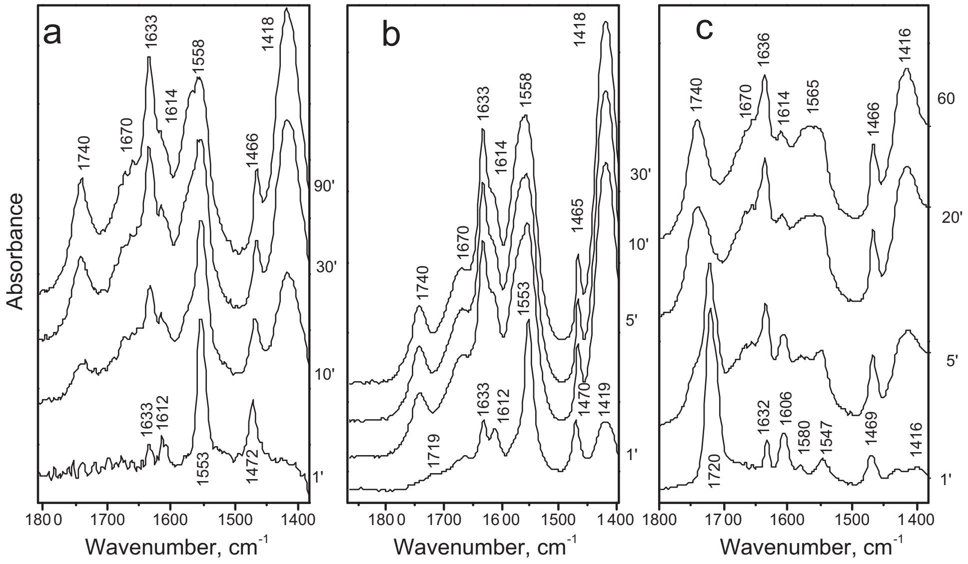

Fig. 13. Difference FTIR spectra collected after the introduction of β-picoline at 200 °C (a) and 250 °C (b) and pyridine-3-carbaldehyde at 160 °C (c) into the cell with VTi-2 catalyst.

the spectrum (Table 2, SC4 and SC6, respectively). With time the intensity of the bands at 1418, 1740 and 1670 cm^{-1} is increased. Two forms of molecular adsorbed nicotinic acid with the similar frequencies in the spectra we have detected after nicotinic acid adsorption on anatase TiO_2 sample containing 6.9 wt.% of sulfate [6].

The transformation of 3-methylpyridinium ion proceeds significantly faster at 250 °C (Fig. 13b), than at 200 °C (Fig. 13a). In addition, the intensity of ν(C=O) band at 1670 cm^{-1} of molecular adsorbed nicotinic acid SC6 is significantly increased. The band at 1719 cm^{-1} assigned to ν(C=O) vibration of pyridine-3-carbaldehyde surface complex SC2 is also observed in the spectrum (Table 2).

The bands at 1720 (ν(C=O)), 1632, 1606, 1580, 1547, 1469 ((ν(CC, CN)), 1416 (ν_s(COO)) cm^{-1} are observed in the FTIR spectrum registered at 160 °C within 1 min after introduction of pyridine-3-carbaldehyde (Fig. 13c). The bands at 1632, 1606, 1547 and 1469 cm^{-1} characterized substituted pyridinium ions. The presence of ν(CC, CN) band at 1580 cm^{-1} in the spectrum indicates the interaction of pyridine-3-carbaldehyde with a Lewis acid centers via an unshared electron pair of nitrogen. Therefore, we can assume that two surface complexes of pyridine-3-carbaldehyde are formed (Table 3, SC2 and SC5). There is also ν_s(COO) band at 1416 cm^{-1} due to nicotinate surface complex in this spectrum (Table 3, SC3). With time the intensity of bands due to pyridine-3-carbaldehyde surface complexes is reduced (primarily band ν(C=O) at 1720 cm^{-1}), whereas the intensity of bands due to nicotinate complex (1565 and 1416 cm^{-1}) is increased. The spectra also contain ν(C=O) bands at 1740 and 1670 cm^{-1} due to molecular adsorbed nicotinic acid (Table 3, SC4 and SC6).

Thus, the same series of surface complexes of similar structure (Tables 2 and 3) and the same sequence of it transformations are observed for both catalysts. However, there are also noticeable differences despite the similarity of the surface structures. Fig. 14 demonstrates the FTIR spectra collected 60 min after introduction of β-picoline in the cell-reactor with VTi-1 (spectrum 1) and VTi-2 (spectrum 2) catalysts at 250 °C. The band at 1670 cm^{-1} due to molecular adsorbed nicotinic acid is appeared in the spectrum of VTi-2 catalyst. The band at 1770 cm^{-1} due to gaseous nicotinic acid is absent in this spectrum. The ratio of intensity of ν(CC, CN) bands at 1633 and ~1610 cm^{-1} is increased in the spectrum of VTi-2. The frequencies of bands assigned to ν_{as}(COO) and ν_s(COO) modes of surface nicotinates are also changed.

The absence of the band at 1770 cm^{-1} of gaseous nicotinic acid in the spectrum 2 could be associated with strong its readsorption on strong Brönsted acid sites of VTi-2 catalyst. In the case of VTi-2 sample the intensity of ν(C=O) band 1740 cm^{-1} due to molecular adsorbed nicotinic acid complex SC4 is increased and molecular adsorbed nicotinic acid complex SC6 (ν(C=O) = 1670 cm^{-1}) is formed. SC6 formation is associated with increase in strength of Brönsted acid sites in the sample VTi-2 due to the presence of sulfate ions on the surface [6] (see also Section 3.1.1). The band

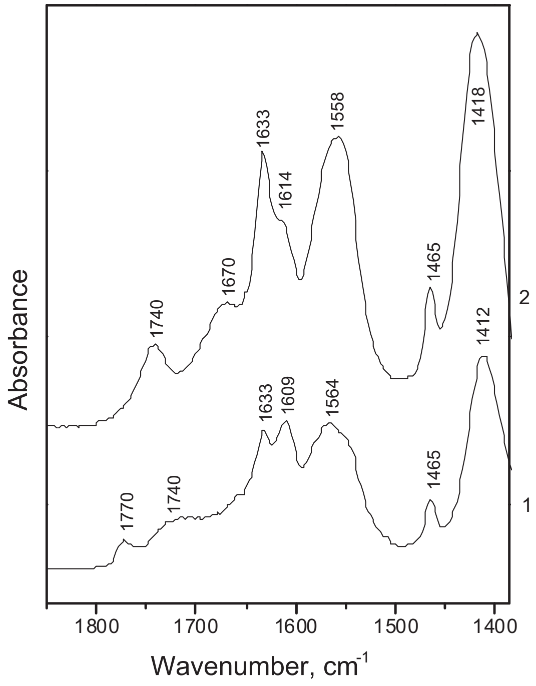

Fig. 14. FTIR spectra collected 60 min after introduction of β-picoline in the cell-reactor with VTi-1 (1) and VTi-2 (2) catalysts at 250 °C.

Table 2
Surface complexes (SC) formed during β-picoline adsorption on VTi-1 and VTi-2.

SC structure	Wavenumbers (cm^{-1}) and band assignment	
	VTi-1	VTi-2
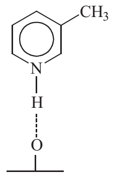 SC1	1632 – ν(CC, CN), 8a 1609 – ν(CC, CN), 8b 1551 – ν(CC, CN), 19a 1470 – ν(CC, CN), 19b 1390 – $\delta(CH_3)$	1633 – ν(CC, CN), 8a 1612 – ν(CC, CN), 8b 1553 – ν(CC, CN), 19a 1472 – ν(CC, CN), 19b
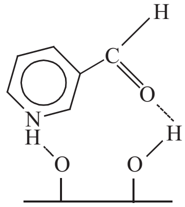 SC2	1720 – ν(C=O)	1719 – ν(C=O)
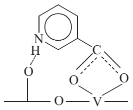 SC3	1633 – ν(CC, CN), 8a 1609 – ν(CC, CN), 8b 1564 – ν_{as}(COO) 1465 – ν(CC, CN), 19b 1412 – ν_s(COO)	1633 – ν(CC, CN), 8a 1614 – ν(CC, CN), 8b 1558 – ν_{as}(COO) 1466 – ν(CC, CN), 19b 1418 – ν_s(COO)
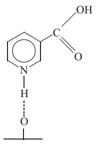 SC4	1740 – ν(C=O)	1740 – ν(C=O)
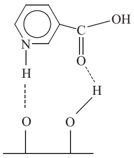 SC6	–	1670 – ν(C=O)

Table 3
Surface complexes (SC) formed during pyridine-3-carbaldehyde adsorption on VTi-1 and VTi-2.

SC structure	Wavenumbers (cm^{-1}) and band assignment	
	VTi-1	VTi-2
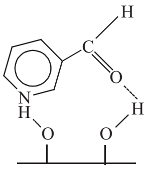 SC2	1721 – ν(C=O) 1631 – ν(CC, CN), 8a 1606 – ν(CC, CN), 8b 1542 – ν(CC, CN), 19a 1468 – ν(CC, CN), 19b	1720 – ν(C=O) 1632 – ν(CC, CN), 8a 1606 – ν(CC, CN), 8b 1547 – ν(CC, CN), 19a 1469 – ν(CC, CN), 19b
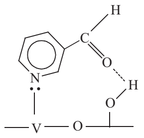 SC5	1721 – ν(C=O) 1578 – ν(CC, CN), 8b	1720 – ν(C=O) 1580 – ν(CC, CN), 8b
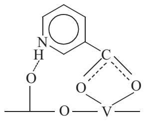 SC3	1633 – ν(CC, CN), 8a 1609 – ν(CC, CN), 8b 1569 – ν_{as}(COO) 1466 – ν(CC, CN), 19b 1411 – ν_s(COO)	1636 – ν(CC, CN), 8a 1614 – ν(CC, CN), 8b 1565 – ν_{as}(COO) 1466 – ν(CC, CN), 19b 1416 – ν_s(COO)
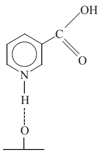 SC4	1740 – ν(C=O)	1740 – ν(C=O)
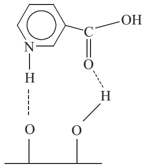 SC6	–	1670 – ν(C=O)

ν(C=O) = 1740 cm^{-1} due to SC4 is observed in the spectra of β-picoline adsorbed on both samples.

Since the frequency of ν(C=O) band in the spectrum of SC4 (1740 cm^{-1}) is close to those in the spectrum of gaseous nicotinic acid (1770 cm^{-1}), carboxyl group of SC4 weakly interacts with acidic sites of the catalyst or do not interacts at all. Thus, this surface complex interacts mainly with the surface via the nitrogen atom of pyridine ring. Proton transfer from a strong Brönsted acid center of the catalyst to the nitrogen atom of nicotinic acid results in the formation of substituted pyridinium ion (complex structure is shown in Tables 2 and 3, SC4). Molecularly adsorbed acid with the frequency of the band ν(C=O) = 1670 cm^{-1} interacts with the Brönsted acid sites of the catalyst both via a nitrogen atom of pyridine ring and via an oxygen atom of the carboxyl group (the structure of the complex is shown in Tables 2 and 3, SC6). The formation of SC6 indicates not only the increase of the strength of the proton centers but also the increase of their surface density. Thus, two-centered interaction between of molecule nicotinic acid and Brönsted centers of the catalyst becomes possible as in the case of highly sulfated anatase [6].

The variation of the ratio of the intensities of ν(CC, CN) bands at 1633 and at ~1610 cm^{-1} in the spectra of surface nicotinate could be due to changing the bonding strength of these complexes with the active centers of the catalyst. The spectrum of nicotinate obtained by transformation of β-picoline on VTi-2 catalyst (Fig. 13, spectrum 2) is similar to the spectrum of nicotinate SC7 formed at pyridine-3-carbaldehyde oxidation on highly sulfated anatase [6]. We have shown in [6] that strongly bound nicotinate SC7 is a dead-end surface complex and it does not turn into nicotinic acid.

It is known that the difference between the frequencies of ν_{as}(COO) and ν_s(COO) vibrations in the IR spectra of salts of carboxylic acids is a structure-sensitive [32,46]. The difference between these frequencies is determined by both the mode of carboxylate ion coordination (mono- or bidentate) and by the strength of the metal-carboxylate bond. Table 4 presents the frequencies of ν_{as}(COO) and ν_s(COO), as well as the value of $\Delta = \nu_{as}(COO) - \nu_s(COO)$ in the spectra of surface nicotinate formed during the transformation of β-picoline on VTi-1 and VTi-2 catalysts.

The frequencies of carboxyl group stretching vibration and the value of Δ indicates bidentate coordination mode of nicotinate

Table 4
The frequencies of ν_{as}(COO) and ν_s(COO) modes, and the value of $\Delta = \nu_{as}(COO) - \nu_s(COO)$ in the spectra of surface nicotinate formed during β-picoline transformation on VTi-1 and VTi-2 catalysts at 250°C.

Catalyst	ν_{as}(COO), cm^{-1}	ν_s(COO), cm^{-1}	Δ, cm^{-1}
VTi-1	1564	1412	152
VTi-2	1558	1418	140

carboxyl group on both samples. It is known [46] that in the case of bidentate coordination mode, increasing the strength of the metal-carboxylate bond reduces the value of Δ. Table 1 shows that the value of Δ for VTi-2 sample is 12 cm^{-1} less than those for VTi-1 sample. Therefore, it is expected that nicotinate stronger bound to VTi-2 surface than to VTi-1 one. It should be noted that the spectra of nicotinic acid adsorbed on VTi-1 and VTi-2 samples at 250 °C (Fig. 15) virtually coincide with the spectra of products of β-picoline and pyridine-3-carbaldehyde transformation on the respective samples (Figs. 11 and 12).

3.1.4. Catalytic properties

The performance of VTi-1 and VTi-2 catalysts in β-picoline oxidation was studied by the thermally programmed reaction method in the temperature range of 240–315 °C (Figs. 16 and 17). The conversion range in this temperature interval was found to be 40–99% for VTi-1 and 40–95% for VTi-2 catalysts. Nicotinic acid, pyridine-3-carbaldehyde, 3-cyanopyridine, pyridine and carbon oxides (CO and CO_2) were found to be the products of β-picoline oxidation on both catalysts. Although nicotinic acid is the main product on both catalysts, their selectivities are different. The maximum nicotinic acid yield is 85% for VTi-1 and less than 50% for VTi-2.

Figs. 18 and 19 demonstrate the dependence of selectivity to reaction products on β-picoline conversion. Nicotinic acid is formed over vanadia–titania catalysts via two pathways. The parallel pathway involves direct β-picoline oxidation. The consecutive mechanism includes the formation of pyridine-3-carbaldehyde as an intermediate [47,48]. The dependence of the selectivities on the β-picoline conversion (Figs. 18 and 19) demonstrates the change in contributions of these pathways depending on the sulfate content. The consecutive nicotinic acid formation pathway predominates on the VTi-1 catalyst: the aldehyde selectivity decreases with increasing β-picoline conversion and the nicotinic acid selectivity simultaneously grows. The contribution of the parallel pathway becomes substantial on the VTi-2 catalyst with high SO_4^{2-} content. It means that adsorption of β-picoline (weak base) is stronger on the catalysts containing more acid sites. The SO_4^{2-} content has even more effect the destiny of pyridine-3-carbaldehyde. It almost completely transforms into nicotinic acid on VTi-1. The contribution of its oxidation to by-products – CO_x, pyridine, 3-cyanopyridine is less than 10% ($\sum S_x - \sum S_0$). On the VTi-2 catalyst the aldehyde is converted only to the side products. This conclusion is proved by the growth of the selectivity to CO_x, pyridine and 3-cyanopyridine with the decrease of the aldehyde selectivity, whereas the nicotinic acid selectivity is not changed.

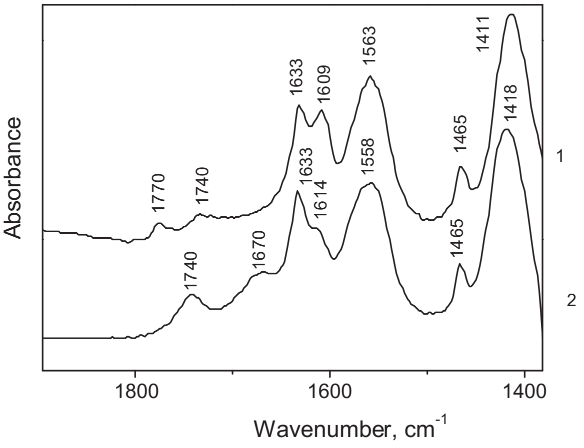

Fig. 15. FTIR spectra of nicotinic acid adsorbed on VTi-1 (1) and VTi-2 (2).

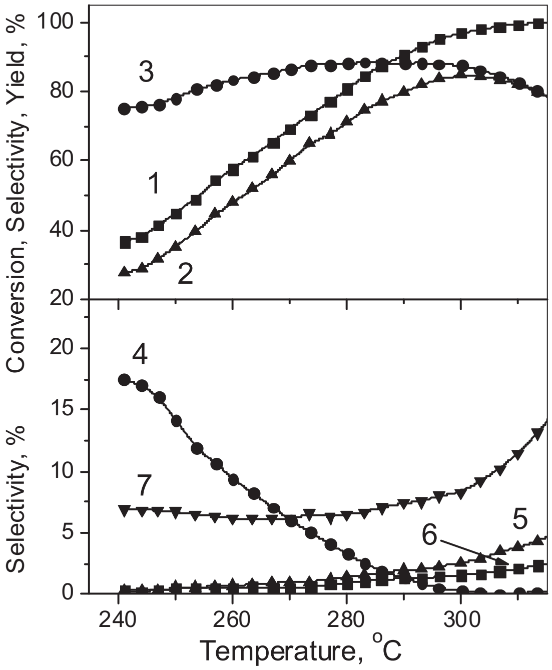

Fig. 16. Temperature dependence of β-picoline conversion (1), nicotinic acid yield (2) and selectivity to nicotinic acid (3), pyridine-3-carbaldehyde (4), 3-cyanopyridine (5), pyridine (6) and CO_x (7) over VTi-1 catalyst.

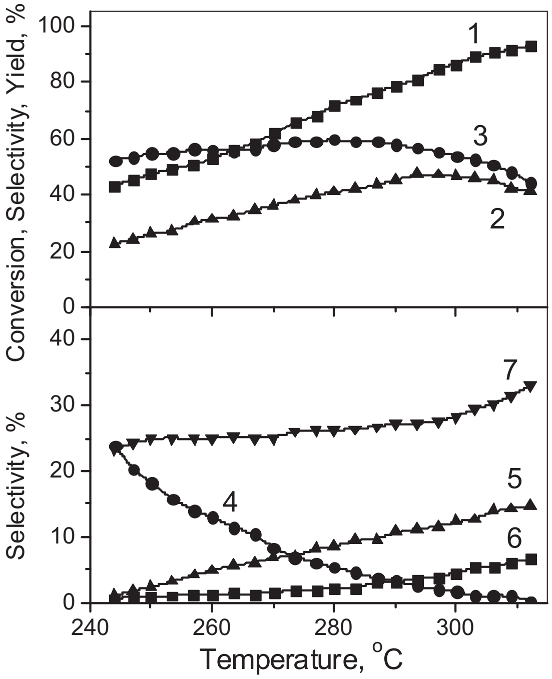

Fig. 17. Temperature dependence of β-picoline conversion (1), nicotinic acid yield (2) and selectivity to nicotinic acid (3), pyridine-3-carbaldehyde (4), 3-cyanopyridine (5), pyridine (6) and CO_x (7) over VTi-2 catalyst.

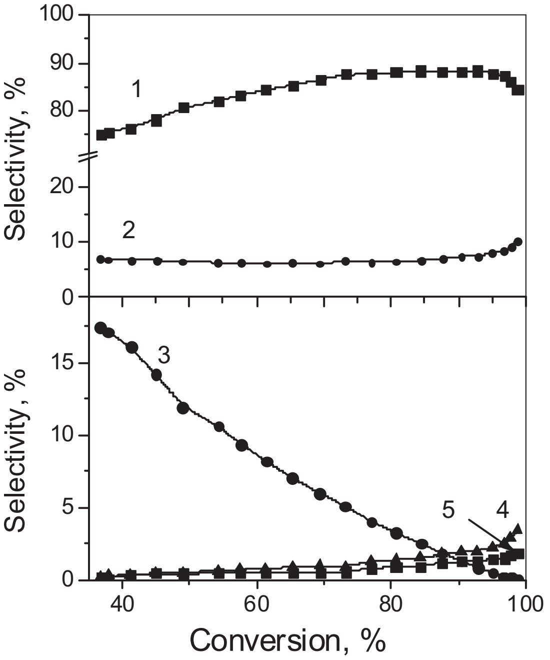

Fig. 18. Dependence of selectivity to nicotinic acid (1), CO_x (2), pyridine-3-carbaldehyde, (3), 3-cyanopyridine, (4) and pyridine (5) upon β-picoline conversion over VTi-1 catalyst.

The observed tendencies are the result of the effect of sulfates on the catalyst acidity. The conception of the acid-base interactions between gaseous reactants and surface acid sites of the solid catalysts was developed by Stair [43]. β-Picoline and pyridine-3-carbaldehyde are organic bases due to the presence of unshared electron pair on the nitrogen atom. Adsorption of these reagents required the presence of acid sites on the surface. The bases interact with such sites by donation of the electron density from the nitrogen atom [43]. Pyridine-3-carbaldehyde is a stronger base than β-picoline due to additional unshared electron pairs on the oxygen atom of the carbonyl group. Both unshared electron pairs on the nitrogen and the oxygen atoms form basic sites that may interact with a pair of acid sites.

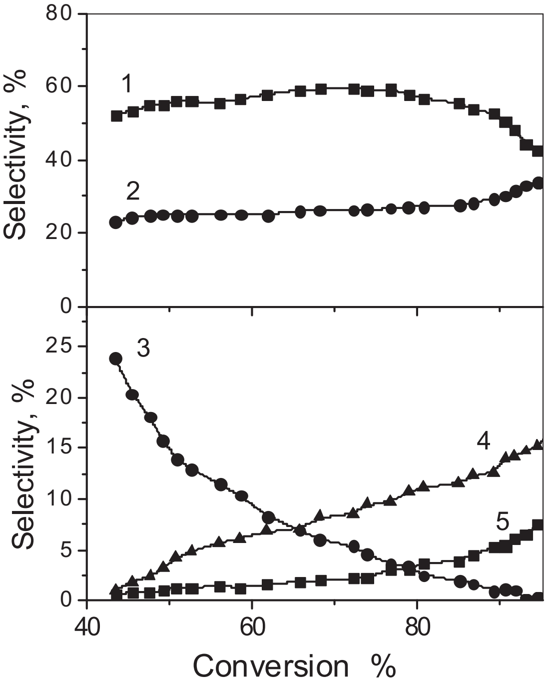

Fig. 19. Dependence of selectivity to nicotinic acid (1), CO_x (2), pyridine-3-carbaldehyde, (3), 3-cyanopyridine, (4) and pyridine (5) upon β-picoline conversion over VTi-2 catalyst.

The introduction of electronegative elements (S^{6+} in our case) onto the surface should produce an inductive effect, making the nearby metal cations less basic or more acidic. The introduction of electropositive species such as alkali metal atoms should produce a more basic or less acidic sites [43]. For instance, the introduction of very electropositive P or Mo atoms to VO_x/SiO_2 decreases the electron density on the vanadium atom making it more acidic. On the contrary, the introduction of potassium results in an increase of the electron density on the vanadium atom leading to stronger basicity [10]. Correlations of the acid-base and catalytic properties of vanadia–titania catalysts promoted with acids or bases have been observed for selective oxidation of o-xylene, toluene, propylene, benzene [8], methanol [49] and methylpyrazine [50,51].

The sulfate content in vanadia–titania catalysts affects the acidity of the active sites, the strength of the surface complexes and directions of their transformations into the reaction products. Growing acidity of the adsorption sites leads to strengthening the surface complexes formed by β-picoline and pyridine-3-carbaldehyde. This effect is stronger for the latter reactant.

The β-picoline adsorption on the very acidic sample VTi-2 results in the formation of strongly bound surface complexes. These complexes are not converted into the pyridine-3-carbaldehyde. Instead, they are transformed following parallel pathways to deeper oxidation products (nicotinic acid and CO_x) and to the products of destruction (pyridine and 3-cyanopyridine). Strongly bound complexes of pyridine-3-carbaldehyde are converted on this catalyst only into the side products. Nicotinates $NC_5H_4COO^-$ are direct precursors of nicotinic acid and also have basic properties. An increase of the catalyst acidity due to the higher SO_4^{2-} content strengthens the nicotinates and decreases the selectivity to nicotinic acid. The transformations of the surface complexes during the temperature increase on the samples with different SO_4^{2-} concentrations confirm described mechanism.

The SO_4^{2-} content also affects further nicotinic oxidation. Though, this effect is less pronounced than the β-picoline and pyridine-3-carbaldehyde transformation to side products. The amount of nicotinic subjected to deeper oxidation is higher on the VTi-2 catalyst. The presence of a nitrogen atom with a unshared electron pair in the pyridine ring determines the stronger reaction of nicotinic acid to the higher amount of stronger acid sites in VTi-2. It results in re-adsorption of the gaseous acid in a stronger form (Fig. 15).

Takehira's assumption [22] on increasing selectivity to nicotinic acid due to its better desorption caused by increasing acidity is not confirmed in the case of highly sulfated vanadium-titanium sample. The negative effect of SO_4^{2-} on the selectivity is likely due to the greater strength of acid sites in the case of VTi catalyst. Unfortunately, we cannot quantitatively compare the effect of acidic centers in VCrP and VTi-SO_4 catalysts since the different methods for the determination of acidity were applied.

Thus, the modification of vanadia–titania catalysts with sulfates increases the catalyst acidity expressed in the strength and concentration of Brönsted acid sites, strengthens the surface complexes of β-picoline, pyridine-3-carbaldehyde and nicotinic acid, and, ultimately, worsens the catalyst characteristics.

4. Conclusion

Strong Brönsted and Lewis acid sites are shown to be present on the surface of vanadia–titania catalysts. The strong Brönsted acid sites on these samples are hydroxyl groups coordinated to vanadium atoms rather than sulfur atoms of sulfate ions. The sulfate ions are coordinated to the same vanadium ions as the hydroxyl groups or to their neighbors. Their presence increases the strength of the Brönsted acid sites. The concentration of strong Brönsted acid sites substantially depends on the water concentration. Water is adsorbed on coordinatively unsaturated vanadium ions (Lewis acid sites) to form Brönsted acid sites.

Vanadia–titania catalysts are efficient in β-picoline oxidation to nicotinic acid. Nicotinic acid is formed via two independent pathways: by direct β-picoline oxidation or through the intermediate pyridine-3-carbaldehyde.

The SO_4^{2-} content in the catalysts affects the strength of the surface complexes and directions of their transformations into the reaction products. An increase of the SO_4^{2-} content results in the higher acidity of Brönsted acid sites, which are the sites where β-picoline and pyridine-3-carbaldehyde are adsorbed. These reagents are weak bases and are adsorbed in a stronger form on the VTi-2 catalyst with higher acidity. The strongly bound surface complexes are transformed into deep oxidation products (CO_x) and products of acid destruction (pyridine and nitrile). Modification of the catalyst with sulfates also favors deep oxidation of nicotinic acid as a result of its re-adsorption.

References

[1] T.V. Andrushkevich, E.V. Ovchinnikova, Catal. Rev.: Sci. Eng. 54 (2012) 399–436, and reference therein.
[2] W.F. Hoelderich, Catal. Today 62 (2000) 115–130.
[3] E.M. Alkaeva, T.V. Andrushkevich, G.A. Zenkovets, M.G. Makarenko, Patent to Bor. Inst. of Catal., RU 2049089 (1995); EP 0747359 A1, WO 9520577 (1995); US 5728837 (1998).
[4] T.V. Andrushkevich, G.Ya. Popova, E.M. Alkaeva, M.G. Makarenko, G.A. Zenkovets, Chem. Ind. 3 (165) (1996) 21–23.
[5] T.V. Andrushkevich, Ind. Catal. News 4 (1998) 4–5 (in Russian).
[6] Yu.A. Chesalov, G.B. Chernobay, T.V. Andrushkevich, J. Mol. Catal. A: Chem. 373 (2013) 96–107.
[7] J.C. Vedrine, Top. Catal. 21 (2002) 1–3.
[8] B. Grzybowska-Swierkosz, Top. Catal. 23 (2002) 35–46.
[9] B. Grzybowska, J. Słoczyński, R. Grabowski, K. Samson, I. Gressel, K. Wcisło, L. Gengembre, Y. Barbaux, Appl. Catal. A: Gen. 230 (2002) 1–10.
[10] A. Klisinska, A. Haras, K. Samson, M. Witko, B. Grzybowska, J. Mol. Catal. A: Chem. 210 (2004) 87–92.
[11] Q. Sun, Y. Fu, J. Liu, A. Auroux, J. Shen, Appl. Catal. A: Gen. 334 (2008) 26–34.
[12] H. Zhao, S. Bennici, J. Cai, J. Shen, A. Auroux, Catal. Today 152 (2010) 70–77.
[13] H. Guo, D. Li, D. Jiang, W. Li, Y. Sun, Catal. Commun. 11 (2010) 396–400.
[14] J. Liu, Q. Sun, Y. Fu, J. Shen, J. Colloid Interface Sci. 335 (2009) 216–221.
[15] T.V. Andrushkevich, Catal. Rev. 35 (1993) 213–259.
[16] T.V. Andrushkevich, Kinet. Catal. 38 (1997) 266–276.
[17] A. Martin, Top. Catal. 29 (2004) 201–204.
[18] L. Kiwi-Minsker, D.A. Bulushev, F. Rainone, A. Renken, J. Mol. Catal. A: Chem. 184 (2002) 223–235.
[19] D.A. Bulushev, F. Rainone, L. Kiwi-Minsker, Catal. Today 96 (2004) 195–203.
[20] V.N. Kalevaru, B.V. Paju, V.V. Pao, A. Martin, Catal. Commun. 9 (2008) 715–720.
[21] K. Takehira, T. Shishido, Z. Song, T. Matsushita, T. Kawabata, K. Takaki, Catal. Today 91–92 (2004) 7–11.
[22] Z. Song, T. Matsushita, T. Shishido, K. Takehira, J. Catal. 218 (2003) 32–41.
[23] H. Zhao, S. Bennici, J. Shen, A. Auroux, Appl. Catal. A: Gen. 356 (2009) 121–128.
[24] H. Zhao, S. Bennici, J. Shen, A. Auroux, J. Catal. 272 (2010) 176–189.
[25] C.-H. Lin, H. Bai, Appl. Catal. B: Environ. 42 (2003) 279–287.
[26] L. Baraket, A. Ghorbel, P. Grange, Appl. Catal. B: Environ. 72 (2007) 37–43.
[27] D. Heinz, W.F. Hölderich, S. Krill, W. Boeck, K. Huthmacher, J. Catal. 192 (2000) 1–10.
[28] D. Heinz, W. Hoelderich, S. Krill, W. Böck, K. Huthmacher, Patent to Degussa, CA2281293 (2000); US 6229018 (2001); EP-984005 (2002).
[29] S.M. Jung, P. Grange, Catal. Today 59 (2000) 305–312.
[30] B. Zhou, D. He, J. Raman Spectrosc. 39 (2008) 1475–1481.
[31] G. Busca, G. Ramis, J.M. Gallardo Amores, V.S. Escribano, P. Piaggio, J. Chem. Soc. Faraday Trans. 90 (1994) 3181–3190.
[32] K. Nakamoto, Infrared and Raman Spectra of Inorganic and Coordination Compounds, fourth ed., A Wiley-Interscience Publication, John Wiley and Sons, New York, Chichester, Brisbane, Toronto, Singapore, 1986.
[33] J.P. Dunn, J.M. Jehng, D.S. Kim, L.E. Briand, H.G. Stenger, I.E. Wachs, J. Phys. Chem. B 102 (1998) 6212–6218.
[34] O. Saur, M. Bensitel, A.B. Mohhamed Saad, J.C. Lavalley, C.P. Tripp, B.A. Morrow, J. Catal. 99 (1986) 104–110.
[35] A. Brückner, U. Bentrup, J.-B. Stelzer, Z. Anorg. Allg. Chem. 631 (2005) 60–66.
[36] G.Ya. Popova, T.V. Andrushkevich, Yu.A. Chesalov, E.V. Ovchinnikova, React. Kinet. Catal. Lett. 87 (2005) 387–394.
[37] E.A. Paukshtis, Infrared Spectroscopy for Heterogeneous Acid Base Catalysis, Nauka, Novosibirsk, 1992.
[38] E. Spinner, J. Chem. Soc. (1963) 3860–3870.
[39] A.A. Tsyganenko, V.N. Filimonov, Spectrosc. Lett. 5 (1972) 477–487.
[40] R. Kourieh, L. Retailleau, S. Bennici, A. Giroir-Fendler, A. Auroux, Catal. Lett. 143 (2013) 74–83.
[41] G.Ya. Popova, Yu.A. Chesalov, T.V. Andrushkevich, React. Kinet. Catal. Lett. 83 (2004) 353–360.
[42] G.B. Chernobay, Yu.A. Chesalov, V.P. Baltakhinov, G.Ya. Popova, T.V. Andrushkevich, Catal. Today 164 (2011) 58–61.
[43] P.C. Stair, J. Am. Chem. Soc. 104 (1982) 4044–4052.
[44] F.-M. Pan, P.C. Stair, Surf. Sci. 177 (1986) 1–13.
[45] M. Johansson, K. Klier, Top. Catal. 4 (1997) 99–108.
[46] M. Kakihana, T. Nagumo, M. Okamoto, H. Kakihana, J. Phys. Chem. 91 (1987) 6128–6136.
[47] E.M. Alkaeva, T.V. Andrushkevich, G.A. Zenkovets, Proceedings of the First World Congress Environmental Catalysis for a Better World and Life, Pisa, Italy, May 1–5, 1995, pp. 447–450.
[48] E.V. Ovchinnikova, T.V. Andrushkevich, React. Kinet. Catal. Lett. 96 (2009) 91–100.
[49] Y. Fu, J. Shen, Chem. Commun. (2007) 2172–2174.
[50] V.M. Bondareva, T.V. Andrushkevich, O.V. Lapina, A.A. Vlasov, L.S. Dovlitova, Catal. Lett. 79 (2003) 164–173.
[51] V.M. Bondareva, T.V. Andrushkevich, O.V. Lapina, A.A. Vlasov, L.S. Dovlitova, E.B. Burgina, Catal. Lett. 78 (2003) 355–363.